

Progress Report on Low-temperature Plasma Science

Center Exchange Program between UCB-OSU

Modeling of surface micro-discharge in humid air with vibrationally excited states of nitrogen

October 8th – October 12th, 2012

Applicant

Dr. Yukinori Sakiyama, Department of Chemical and Biomolecular Engineering, University of California at Berkeley

E-mail: ysaki@berkeley.edu

Principal Investigators

Prof. David Graves, Department of Chemical and Biomolecular Engineering, University of California at Berkeley

Prof. Igor Adamovich, Department of Mechanical and Aerospace Engineering, Ohio State University

1. Introduction

Surface micro-discharge (SMD) [1] is one type of surface dielectric barrier discharge (DBD) operating in ambient air at or near room temperature. The SMD device consists of a planar powered metal electrode and mesh grounded electrode with dielectric material between the electrodes. The primary application of SMD plasmas is biomedicine. Various publications demonstrated the strong bactericidal effects from using this type of device [2][3]. Treated surfaces are normally located a few centimeters away from the SMD device. Therefore, relatively long-lived reactive oxygen and nitrogen species (RONS) are thought to play the primary role in the observed biological effects. We have developed a global model of SMD plasmas with extensive chemical reaction mechanisms to identify RONS generated by SMD plasmas [4]. Major RONS obtained by the numerical model at relatively low power (0.05 W/cm^2) include O_3 , N_2O_5 , N_2O , and HNO_3 . The simulation results showed qualitative agreement with FTIR measurement. Our recent measurement showed that distribution of the RONS is quite dynamic in time. For instance, the discharge mode transits from ‘ O_3 mode’ to ‘ N_xO_y mode’ at a fixed input power [5]. In addition, the distributions depend on electrode temperature and presence of aqueous phase [6]. Interestingly, our numerical model failed to reproduce the observed mode transition. A most plausible explanation is that the generation rate of NO was significantly underestimated in the current model. Previous publications [7][8] suggest that vibrationally excited nitrogen ($\text{N}_2(v)$) is a key to generate NO, which was not included in the model.

The aim of this joint collaboration between Graves group in University of California at Berkeley (UCB) and Adomovich group in Ohio State University (OSU) was to add vibrationally excited states of nitrogen in the numerical model developed at UCB and discuss possible mechanisms of the observed dynamic behavior of SMD plasmas. In the following sections, we describe the model and report the preliminary simulation results.

2. Description of the model

The simulation domain, discharge conditions, governing equations, and reaction mechanisms are identical to the previous report [4]. The simulation domain consists of two, coupled well-mixed regions of discharge layer and afterglow. The thickness of the discharge layer is 0.1 mm and the width of the afterglow region is 10 mm. A Gaussian-like electric field pulse is excited at 10 kHz with full width at half maximum of 10 ns in the discharge layer. The amplitude of the pulse electric field is adjusted to maintain the period-averaged power density in the discharge layer. The model takes into account 53 chemical species and 624 reactions in humid air. Multiple time-step approach is used to keep track of transient behavior of SMD-generated species for tens of minutes after SMD ignition, while resolving the pulsed electric field and resultant reaction of electrons and ions. An ODE solver in MATLAB [9] is used to solve 53 ordinary differential equations (ODE) in both domains.

We have added a conservation equation for vibrational energy density of nitrogen ($E_v = \varepsilon_v n_{N_2}$) to the SMD model mentioned above, based on an assumption that vibrational energy distribution follows a Maxwell-Boltzmann distribution.

$$\frac{dE_v}{dt} = k_{eV} n_e n_{N_2} - (E_v - E_{v_0}) / \tau_{VT} - \varepsilon_v k_{625} F_{v>12} n_O n_{N_2}, \quad (1)$$

where ε_v is mean vibrational energy, n_{N_2} is nitrogen density, k_{eV} is rate of electron impact excitation of vibrational energy. k_{eV} is obtained by solving Boltzmann equation of electron energy distribution function. E_{v_0} and τ_{VT} are the ground state vibrational energy density and vibration energy relaxation time, respectively. k_{625} is reaction rate of the generation of NO and N from $N_2(v)$ and O. $F_{v>12}$ is cumulative distribution function with higher vibrational states than 12th state.

$$F_{v>12} = \exp\left(-\frac{12\Delta\varepsilon_v}{k_b T_v}\right). \quad (2)$$

$\Delta\varepsilon_v$ is 0.29 eV, k_b is Boltzmann constant. T_v is vibrational temperature and obtained by vibrational energy ε_v using the following relation.

$$T_v = \frac{\Delta\varepsilon_v}{k_b \ln(\Delta\varepsilon_v/\varepsilon_v + 1)}. \quad (3)$$

On the right-hand side of equation (1), the first term represents electron impact excitation. The second and the third terms are collisional quenching and inelastic loss rate, respectively. The relaxation rate (τ_{vT}^{-1}) is given as sum of quenching rate by three species: N_2 , O, and H_2O [10][11][12].

$$1/\tau_{vT} = 1/\tau_{N_2} + 1/\tau_O + 1/\tau_{H_2O}, \quad (4)$$

$$1/\tau_{N_2} = 1.54 \times 10^3 \exp(-137/T_g^{1/3}) n_{N_2} k T_g, \quad (5)$$

$$1/\tau_O = 1.07 \times 10^{-16} \exp(-69.9/T_g^{1/3}) n_O, \quad (6)$$

$$1/\tau_{H_2O} = 1.2 \times 10^{-20} n_{H_2O} \quad (7)$$

T_g is gas temperature (translational and rotational temperature) and n_{H_2O} is density of water vapor. The vibrational energy density equation is solved in both discharge layer and afterglow region. Vibrational energy density diffuses between the two regions as do other long-lived species, while no electron impact excitation occurs in the afterglow region.

We note that the *actual* vibrational distribution function is most likely non-Maxwellian under conditions considered here [13]. A state-to-state model could provide more accurate results. However, the state-to-state model requires more intensive computational resources. Also, not all the parameters used in the state-to-state approach are known. Therefore, we begin this study with the simplified model solving vibrational energy density in order to investigate the effects of $N_2(v)$

in a semi-quantitative manner.

3. Results and discussion

Figures 1 show time-development of vibration temperature in the two regions and selected major species in the afterglow region. Gas temperature is fixed at 300 K in both regions. The ‘background’ gas consists of 79% N₂, 20% O₂, and 1% H₂O. The discharge power is 0.5 W/cm². In our UV absorption spectroscopy at the same power density, observed ozone density was less than our detection limit (10 ppm = $\sim 10^{20}$ m⁻³) [5]. In our numerical simulation, however, ozone density reaches $\sim 2.5\%$ ($\sim 25,000$ ppm) of the background gas and remains almost constant for 1000 s as shown in figure 1 (b). Although N_xO_y gradually build up, the density is still lower than O₃ by a factor of 2-3. The ‘ozone poisoning’ (i.e. reduction of ozone concentration) was not observed in our simulation. Figure 1 (a) shows that vibrational temperature remains low (~ 600 K) under the condition considered here. Our preliminary estimation indicated that vibrational temperature needs to be at least 2,000-3,000 K in the discharge layer in order to destroy O₃ by NO generated by N₂(*v*) and O.

Possible explanations of the discrepancy between the experiment and simulation are as follows: (a) increase in gas temperature plays a role (e.g. thermal decomposition), (b) the loss term in equation (1) is overestimated, (c) the generation term in equation (1) is underestimated, and (d) the assumption of Maxwell distribution is so far from validity that it has affected the results qualitatively. In order to investigate the scenarios (a) and (b), we carried out simulations by modulating input parameters. The rest of the scenarios will be investigated in the near future.

As for scenario (a), we observed the electrode temperature increases by ~ 30 -40 K when the SMD device operates at 0.5 W/cm² for ~ 10 min. Our preliminary estimation suggests that gas temperature in the discharge layer can reach ~ 350 K under that condition. Figure 2 plots the

time-evolution of long-lived species in the afterglow when gas temperature in the discharge layer is fixed to 350 K, instead of 300 K. We see no difference in calculated vibrational temperature from figure 1 (a) although we do not show the data here. Figure 2 indicates that O₃ is decomposed by gas heating and the density reduces by a factor of ~3. However, ozone density still remains around 0.8% (~8000 ppm), which is much higher than our experimental observation (<10 ppm) at 0.5 W/cm². We considered the possibility that our model assumption of a uniform gas temperature is wrong. Gas temperature could respond locally to each filamentary-like micro-discharge and increase for a short period of time every 100 μs. In this scenario, instantaneous peak temperature could be significantly higher than the measured phase-averaged temperature. However, our preliminary calculation by solving the energy balance equation indicates that the instantaneous temperature increase is ~5 K. Therefore we think localized gas heating is not the dominant factor to explain the observed O₃ destruction. We plan to measure optical emission spectra from nitrogen excited states and infer rotational (and therefore translational) temperature to verify our argument.

The dominant loss mechanism of nitrogen vibrational energy is probably collisional quenching by H₂O. In figures 1, we assumed 1% of H₂O in the background gas (~30% relative humidity at room temperature). The characteristic time of the quenching is ~1 ms under that condition (Eq. (7)). We carried out a simulation with dry air in order to investigate the effect of humidity on the distribution of RONS in the afterglow region. Figure 3 (a) shows that vibrational temperature increases over 5000 K in the discharge layer when ambient air is completely dry.. As a result, O₃ is destroyed and NO and NO₂ become dominant as shown in figure 3 (b). Of course, the experiment was in fact conducted in ambient air with non-zero humidity. Therefore, figures 3 cannot be used to fully explain the experimental result in which O₃ was less than our detection limit. However, figures 3 clearly showed that the model indicates that the kinetics of quenching from water vapor can strongly alter the distributions of RONS. We will run simulations under different humidity and

investigate the influence to the distributions of RONS. It is also possible that a more accurate state-to-state treatment of the water vapor quenching kinetics could explain the measurements.

4. Concluding remarks

We modified our global model of SMD and added the vibrational energy density equation of nitrogen to the model. The modified model showed that elevated gas temperature appears not to be the primary factor affecting the observed ozone concentration changes with power. In addition, our simulation results indicated that kinetic processes associated with gas humidity has a major impact on the distributions of RONS. We will further investigate potential mechanisms, including other NO generation mechanisms involving electronically excited states of nitrogen [14] and influence of non-Maxwell distributions.

References

- [1] Morfill G E, Shimizu T, Steffes B and Schmidt H-U 2009 *New J. Phys.* **11** 115019
- [2] Zimmermann J L, Dumler K, Shimizu T, Morfill G E, Wolf A, Boxhammer V, Schlegel J, Gansbacher B and Anton M 2011 *J. Phys. D.* **44** 505201
- [3] Traylor M J, Pavlovich M J, Karim S, Hait P, Sakiyama Y, Clark D S and Graves D B 2011 *J Phys. D* **44** 472001
- [4] Sakiyama Y, Graves D B, Chang H-W, Shimizu T, and Morfill G E 2012 *J. Phys. D.* **45** 425201
- [5] Shimizu T, Sakiyama Y, Graves D B, Zimmermann J L and Morfill G E *New J. Phys.* (in print)
- [6] Shimizu T, Sakiyama Y, Chang H-W, Graves D B, Zimmermann J L and Morfill G E (in preparation)

- [7] Capitelli M, Ferreira C M, Gordiets B F and Osipov A I 2000 *Plasma Kinetics in Atmospheric Gases* (Berlin: Springer)
- [8] Fridman A 2008 *Plasma Chemistry* (New York: Cambridge University Press)
- [9] MATLAB 7.11 2010 (Natick, MA: Mathworks)
- [10] Mnatsakanyan A K and Naidis G V 1985 *High Temp.* **23** 506
- [11] Taylor R L 1974 *Can. J. Chem.* **52** 1436
- [12] Whitson Jr. M E and McNeal R J 1977 *J. Chem Phys.* **66** 2696
- [13] Adamovich I V, Macheret S O and Rich J W 1994 *Chemical Physics* **182** 167
- [14] Uddi M, Jiang N, Adamovich I V and Lempert W R 2009 *J. Phys. D* **42** 075205

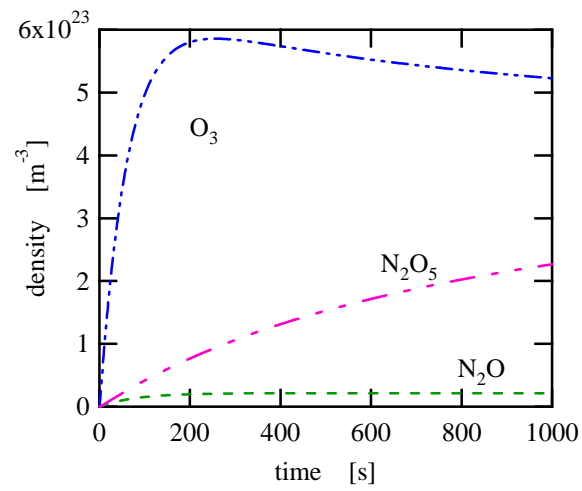
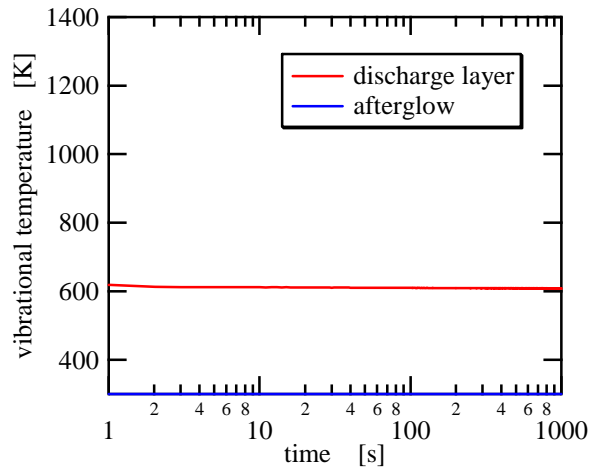


Figure 1 Simulation results at 0.5 W/cm^2 with 1% H_2O . Gas temperature is 300 K. (a) vibrational temperature obtained by the modified model and (b) distributions of major species in the discharge layer.

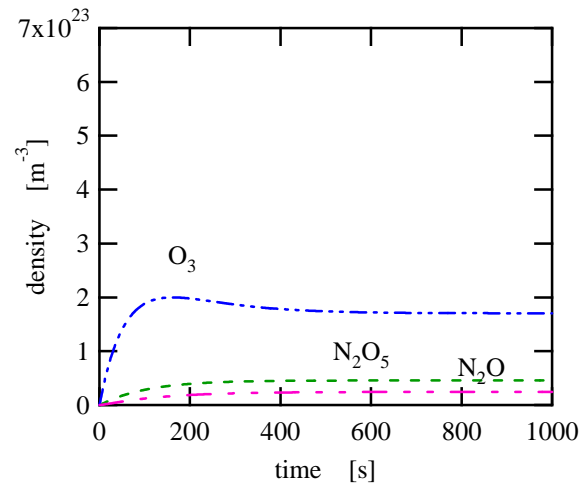


Figure 2 Simulation results at 0.5 W/cm^2 with 1% H_2O . Gas temperature in the discharge layer is 350 K and that in the afterglow region is at 300 K.

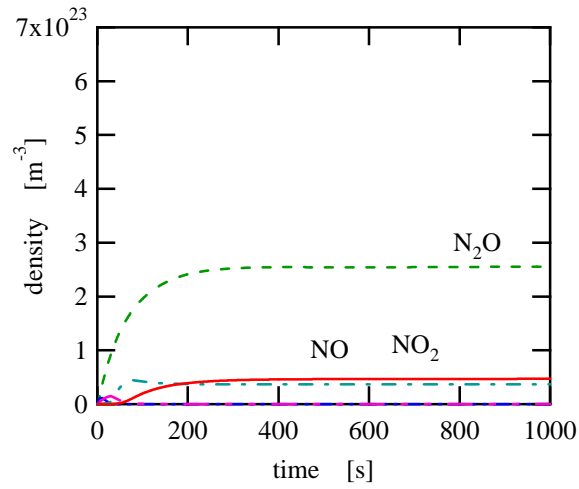
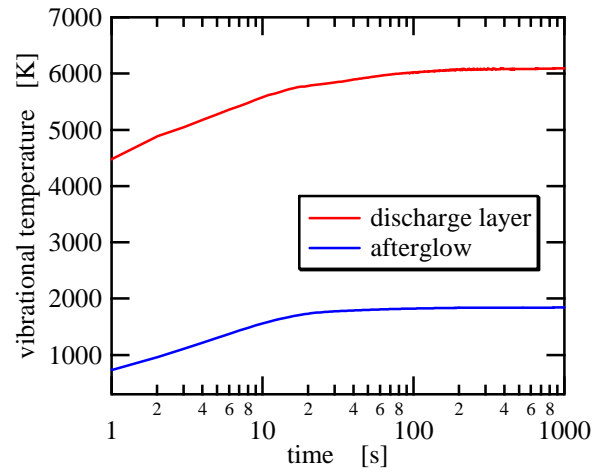


Figure 3 Simulation results at 0.5 W/cm^2 without H_2O . Gas temperature is 300 K. (a) vibrational temperature obtained by the modified model and (b) distributions of major species in the discharge layer.